

Preparation and photocatalytic activity of boron-modified TiO₂ under UV and visible light

Adriana Zaleska ^{a,*}, Janusz W. Sobczak ^b, Ewelina Grabowska ^a, Jan Hupka ^a

^a Department of Chemical Technology, Gdańsk University of Technology, 80-952 Gdańsk, Poland

^b Laboratory of Electron Spectroscopies, Institute of Physical Chemistry Polish Academy of Sciences, 01-224 Warsaw, Poland

Received 8 July 2007; received in revised form 5 September 2007; accepted 9 September 2007

Available online 14 September 2007

Abstract

Synthesis of new boron-containing TiO₂ powders (B-TiO₂) and their activity under UV and visible light are reported. The catalysts were prepared by the sol-gel method and by grinding anatase powder with a dopant. Boric acid triethyl ester and boric acid were used as boron sources in both catalysts preparation procedures. The photocatalytic activity of obtained powders in UV and visible light was estimated by measuring the decomposition rate of phenol (0.21 mmol/dm³) in an aqueous solution. Carbon and boron presence in all prepared photocatalysts was confirmed by the XPS technique. The oxidation state of B atoms incorporated in TiO₂ particles was mainly B³⁺, as determined from the X-ray photoelectron spectra (XPS). It was confirmed that boron-doped TiO₂ was activated by visible light and used as effective catalyst in photooxidation reactions.

© 2007 Elsevier B.V. All rights reserved.

Keywords: Titanium dioxide; Boron-doped TiO₂; Visible light

1. Introduction

Strong oxidation and reduction power of photoexcited titanium dioxide was realized from the discovery of Honda-Fujishima effect. In 1972, Fujishima and Honda [1] reported photoinduced decomposition of water on TiO₂ electrodes. Since Frank and Bard [2] first examined the possibilities of using TiO₂ to decompose cyanide in water, there has been an increasing interest in environmental applications. Based on these works, TiO₂ photocatalysts are widely used for air purification, deodorization, sterilization, anti-fouling, and mist removal [3,4]. The pristine TiO₂ is only active upon ultraviolet light ($\lambda < 387$ nm) because of its band gap (3.2 eV in the anatase TiO₂ crystalline phase). To improve the photocatalytic reactivity of TiO₂ and to extend its light absorption into the visible region transition metal doping [5–8] and reduced forms of TiO_x [9,10] were proposed. Nevertheless, such catalysts did not show long-term stability and had limited levels of activity considering their applications. Recently, some research groups demonstrated methods of substitution of non-metal atoms, such

as nitrogen [11–15] and sulfur [16–19] for oxygen in the lattice of TiO₂. Asashi et al. [11] synthesized N-doped TiO₂ by sputtering the TiO₂ target in N₂/Ar mixture. Diwald et al. [20] prepared nitrogen-doped rutile by thermal treating of a single TiO₂ crystal in NH₃ atmosphere. Ohno et al. [21] reported synthesis of S-TiO₂ photocatalyst prepared by hydrolysis of titanium isopropoxide in the presence of thiourea. Visible-light activated titanium dioxide photocatalysts obtained by hydrolysis of titanium (IV) isopropoxide with thioacetamide or thiourea, followed by calcinations at 450 °C were also reported by us earlier [22].

Considering more theoretical approach, Xu et al. [23] studied the band structure of nitrogen (N)-, carbon (C)- and boron (B)-doped titanium dioxide by first-principles quantum mechanics calculation performed using local-density approximation (LDA). The band gap calculated by this method was 2.33, 2.44, 2.85 and 2.47 eV for N-, C-, B-doped TiO₂ and pure TiO₂, respectively. Their study showed that three 2p bands of impurity atom are located above the valence-band maximum and below the Ti 3d bands, and that along with the decreasing impurity atomic number, the fluctuations become more intensive. They could not observe obvious band-gap narrowing in their results. Therefore, the cause of absorption in visible light might be the isolated impurity atom 2p states in band-gap

* Corresponding author. Tel.: +48 58 3472437; fax: +48 58 3472065.

E-mail address: azal@chem.pg.gda.pl (A. Zaleska).

rather than the band-gap narrowing [23]. Geometric and electronic structures of the boron-doped TiO_2 photocatalyst were estimated by Geng et al. [24] by calculation with a plane-wave-based pseudo-potential method. They found that boron-doped anatase occurred to be much more efficient and stable photocatalyst than the pristine TiO_2 . Moon et al. [25] confirmed, in a laboratory experiment, that modification of TiO_2 with boron oxides is very effective for photocatalytic decomposition of water under UV light. They observed that B- TiO_2 photocatalysts decomposed water stoichiometrically in aqueous suspension system [25]. Zhao et al. [26] improved appreciably the photocatalytic efficiency by doping TiO_2 simultaneously with boron atom and nickel oxide, Ni_2O_3 , thus extending the absorption spectrum to the visible region [26]. Photoactivity of B- TiO_2 nanoparticles under UV light was also investigated by Chen et al. [27]. Chen et al. synthesized B-doped TiO_2 with different atomic ratios of B to Ti (from 1 to 20%) by sol-gel method followed by calcination at 500–800 °C, using boric acid as a boron source.

TiO_2 doped by non-metals, by carbon, sulfur and nitrogen, was extensively investigated as vis-activated photocatalyst. Based on theoretical calculations, boron appears as another non-metal dopant for titanium dioxide modification, but B- TiO_2 activity in visible light has not been investigated. In this work, we present detailed data on photocatalytic activity under UV and visible light of new boron-doped TiO_2 powders. The powders were prepared according to two different procedures: by the sol-gel method and by grinding anatase powder with a dopant containing boron. Boric acid triethyl ester ($\text{C}_2\text{H}_5\text{O}$)₃B and boric acid (H_3BO_3) were used as boron source in both catalyst preparation procedures.

2. Experimental section

2.1. Materials and instruments

Titanium (IV) isopropoxide (97%) was obtained from Aldrich Chem. Co. TiO_2 ST-01 powder having anatase crystal structure was obtained from Ishihara Sangyo, Japan. ST-01 has a specific surface area 300 m^2/g with particle size 7 nm. Boric acid triethyl ester (99%) and boric acid (99%) from Sigma-Aldrich Co. were used as boron source in both catalysts' preparation procedures without further purification. B_2O_3 powder was obtained from Sigma-Aldrich Co.

Areameter II instrument (Strohlein) was used for measurements of BET surface area of the catalysts. The S_{BET} values were calculated according to the BET method using adsorption data at relative pressures p/p_0 between 0.05 and 0.25, where p and p_0 denote the equilibrium pressure.

The catalyst powder crystal structure was determined from XRD pattern measured in the range of $2\theta = 20\text{--}80^\circ$ using X-ray diffractometer (Xpert PRO-MPD, Philips) with Cu target K α -ray ($\lambda = 1.5404 \text{ \AA}$). The diffuse absorption spectra DRS were characterized using UV-vis spectrometer (Specord M40, Carl Zeiss) equipped with an integrating sphere accessory for diffuse reflectance.

ESCALAB-210 spectrometer (VG Scientific) was used for X-ray photoelectron spectroscopy (XPS) measurements with the Al K α X-ray source operated at 300 W (15 kV, 20 mA). The spectrometer chamber pressure was about 5×10^{-9} mbar. The samples were pressed into pellets before measurements. Survey spectra were recorded for all the samples in the energy range from 0 to 1350 eV with 0.4 eV step. High-resolution spectra were recorded with 0.1 eV step, 100 ms dwell time and 20 eV pass energy. 90° take-off angle was used in all measurements. AVANTAGE data system software served for curve fitting. The background was fit using nonlinear Shirley model. Scofield sensitivity factors and measured transmission function were used for quantification. Carbon contamination C1s peak at 284.60 eV was used as reference of binding energy.

2.2. Preparation of B- TiO_2 photocatalyst

In the sol-gel method, B-doped TiO_2 catalysts were prepared from titanium (IV) isopropoxide, known to be the titanium source origin for anatase-type TiO_2 . A sample of 10 cm³ of titanium (IV) isopropoxide (TIP) solution (97%, Sigma-Aldrich) in isopropanol (3.74 ml) was mixed with 0.073 and 1.46 g of boric acid (0.5 or 10% B) or with 0.2, 0.4, 1, and 2 ml of boric acid triethyl ester (0.5, 1, 5 or 10% B). 2.35 ml of deionized water were added dropwise into the solution. The solution was stirred for 1 h and subsequently kept at room temperature for 2 weeks until white powder was obtained. The resulting powders were dried for 96 h at 80 °C and then calcinated at 450 °C for 1 h. The heating rate was 15 °C/min.

In the second procedure boron-modified TiO_2 powders were prepared by grinding 3 g of ST-01 in an agate mortar with 0.084 and 1.69 g of boric acid and 0.23 and 4.7 ml of boric acid triethyl ester, respectively. Obtained powders were dried for 24 h at temperature 80 °C and calcinated at 450 °C. The resulting powders were labeled as B-E for boric acid triethyl ester and B-A for boric acid as boron precursors.

2.3. Photocatalytic decomposition of phenol

The photocatalytic activity of B- TiO_2 powders in ultraviolet and visible light was estimated by measuring the decomposition rate of phenol (0.21 mmol/dm³) in an aqueous solution. Photocatalytic degradation runs were preceded by blind tests in the absence of a catalyst or illumination.

Twenty five millilitres of catalyst suspension (125 mg) was stirred using magnetic stirrer and aerated (5 dm³/h) prior and during the photocatalytic process. Aliquots of 1.0 cm³ of the aqueous suspension were collected at regular time periods during irradiation and filtered through syringe filters ($\phi = 0.2 \mu\text{m}$) to remove catalyst particles. Phenol concentration was estimated by colorimetric method using UV-vis spectrophotometer (DU-7, Beckman). The suspension was irradiated using 1000 W Xenon lamp (Oriel), which emits both UV and vis light. To limit the irradiation wavelength, the light beam was passed through GG400 or UG11 filter to cut-off wavelengths shorter than 400 nm or $250 < \lambda < 400 \text{ nm}$, respectively.

Table 1

Characteristics of B-TiO₂ catalysts synthesized by TIP hydrolysis and grinding in the presence of boric acid triethyl ester and boric acid

Sample no.	Type of synthesis	Kind of dopant	TiO ₂ :dopant molar ratio	Assumed content of boron (wt.%)	Band-gap energy (eV)	Phase composition	BET surface area (m ² /g)
BE-H(0.5)	Sol-gel	(C ₂ H ₅ O) ₃ B	1:0.036	0.5	3.28	Amorphous	208
BE-H(1)	Sol-gel	(C ₂ H ₅ O) ₃ B	1:0.072	1	3.37	Amorphous	237
BE-H(5)	Sol-gel	(C ₂ H ₅ O) ₃ B	1:0.36	5	3.41	Amorphous	269
BE-H(10)	Sol-gel	(C ₂ H ₅ O) ₃ B	1:0.72	10	3.36	Amorphous	190
BE-G(0.5)	Grinding	(C ₂ H ₅ O) ₃ B	1:0.037	0.5	3.36	Anatase	160
BE-G(10)	Grinding	(C ₂ H ₅ O) ₃ B	1:0.74	10	3.37	Anatase + B ₂ O ₃	158
BA-H(0.5)	Sol-gel	H ₃ BO ₃	1:0.04	0.5	3.34	Anatase	219
BA-H(10)	Sol-gel	H ₃ BO ₃	1:0.72	10	3.40	Amorphous	330
BA-G(0.5)	Grinding	H ₃ BO ₃	1:0.04	0.5	3.30	Anatase	163
BA-G(10)	Grinding	H ₃ BO ₃	1:0.72	10	3.33	Anatase + B ₂ O ₃	82
Pure TiO ₂	Sol-gel	No dopant	—	0	3.29	Anatase	180
TiO ₂ ST-01	—	No dopant	—	0	3.30	Anatase	211

3. Results and discussion

The amount of the dopant taken for catalyst preparation was calculated on the assumption that the content of boron in the catalyst after synthesis should be equal from 0.5 to 10 wt.% of the catalyst dry mass. Sample numbers, the amount of the dopant used during preparation and measured band-gap energies (E_g) value are presented in Table 1. All the catalysts obtained in this work were in the form of beige powders, except sample BE-H(10), which appeared in dark-brownish color. The band-gap energy (E_g) determination was based on numerical derivative of the optical absorption coefficient. For pure TiO₂ prepared by hydrolysis without any dopant and for TiO₂ ST-01, the E_g was 3.29 and 3.30 eV, respectively. In the case of B-TiO₂ modified with boric acid triethyl ester, E_g increased to 3.41 eV depending on the dopant amount. For TiO₂ modified with boric acid triethyl ester by grinding, E_g was in range 3.36–3.37 eV. Band gap for B-TiO₂ modified with boric acid fluctuated from 3.30 to 3.40 eV. The highest E_g was observed for sample BE-H(5) prepared by sol-gel method using 5 wt.% of boric acid triethyl ester (see Table 1). We did not observe band-gap narrowing in B-TiO₂, which is in good agreement with theoretical calculation made by Xu et al. [23]. The band-gap

energy value calculated by Xu et al. [23] for anatase equals 2.47 eV, less than the experimental value usually reported for anatase in the literature (~3.2 eV). It is due to well-known underestimation of the LDA method. Calculated E_g value for B-TiO₂ is 2.85 eV, which is 0.38 eV larger than that of pure TiO₂. For our samples the average difference between E_g of pristine and boron-doped TiO₂ equals to 0.06 eV and it depends on the amount of the used dopant. Broadening of band gap according to Xu et al. [23] results from low or no mixing of 2p boron bands with 2p oxygen bands, because the matching of p bands decreases along with the difference in electronegativity.

Figs. 1 and 2 show absorption spectra of B-TiO₂ doped with boric acid triethyl ester prepared by hydrolysis of TIP and by grinding of ST-01 with a dopant. The best photoabsorption in the visible region can be attributed to the BE-H(10) obtained by sol-gel method in the presence of boric acid triethyl ester. We did not observe a red shift for boron-doped photocatalysts but some samples show lack of sharp absorption edge as observed for pure TiO₂.

Figs. 3 and 4 show the absorption spectra of B-TiO₂ doped with boric acid prepared by hydrolysis of TIP and by grinding of ST-01 with a dopant. There is no difference in absorption for samples modified with 0.5 wt.% of boric acid and pure TiO₂.

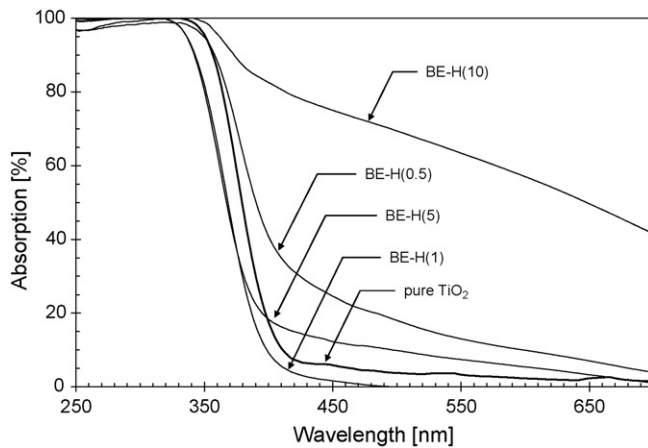


Fig. 1. Diffuse reflectance spectra of pure and B-doped prepared by hydrolysis of TIP in the presence of (C₂H₅O)₃B.

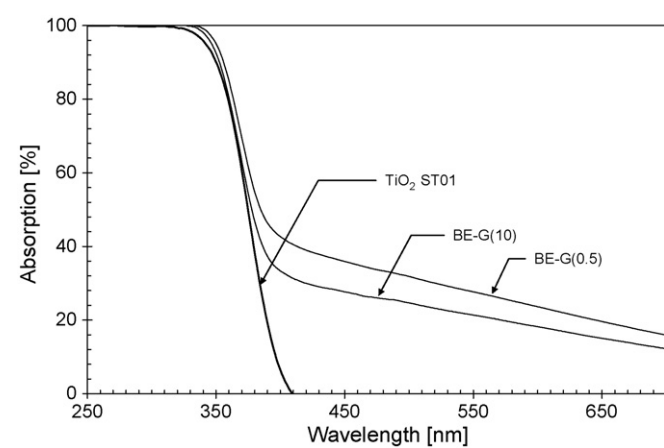


Fig. 2. Diffuse reflectance spectra of TiO₂ ST-01 and B-doped prepared by grinding anatase with (C₂H₅O)₃B.

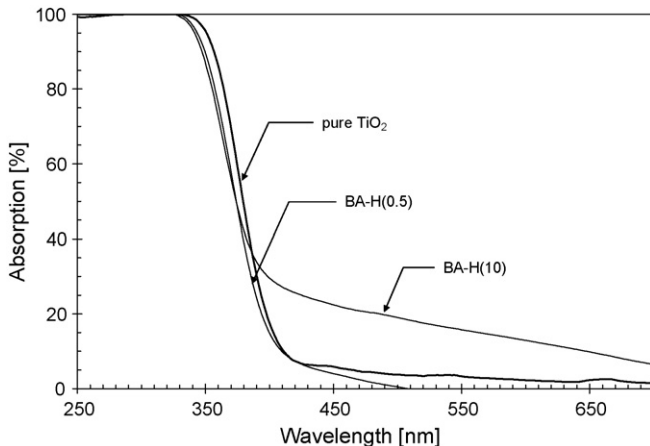


Fig. 3. Diffuse reflectance spectra of pure and B-doped prepared by hydrolysis of TIP in the presence of H₃BO₃.

Stronger absorption is observed for samples BA-H(10) and BA-G(10), prepared with bigger amount of H₃BO₃. Samples modified with boric acid triethyl ester revealed stronger absorption in visible region than samples modified with boric acid, assuming the same amount of boron introduced to the TiO₂ structure.

To obtain information on the crystal structure of the B-TiO₂ photocatalysts, X-ray diffraction patterns were measured, see data on crystalline phase in Table 1. Fig. 5 shows the XRD patterns of selected B-TiO₂ photocatalysts as well as pure TiO₂, and diboron trioxide as a reference. All samples obtained by the sol–gel method, except sample BA-H(0.5), appeared as amorphous TiO₂, while pure TiO₂ obtained by the same method without any dopant was in the anatase form. Addition of (C₂H₅O)₃B or H₃BO₃ inhibited crystallite growth and/or transformation from amorphous to anatase structure. Only addition of smallest amount of H₃BO₃ (0.5 wt.%), resulted in anatase structure, see Fig. 5. Chen et al. [27], reported that boron doping inhibited grain growth and facilitated anatase-to-rutile transformation. They found, that the average crystallite size for B-TiO₂ calcinated at 500 °C decreased from 15 to 9, as the molar ratio of B to Ti (R_B) increased from 0 to 20.

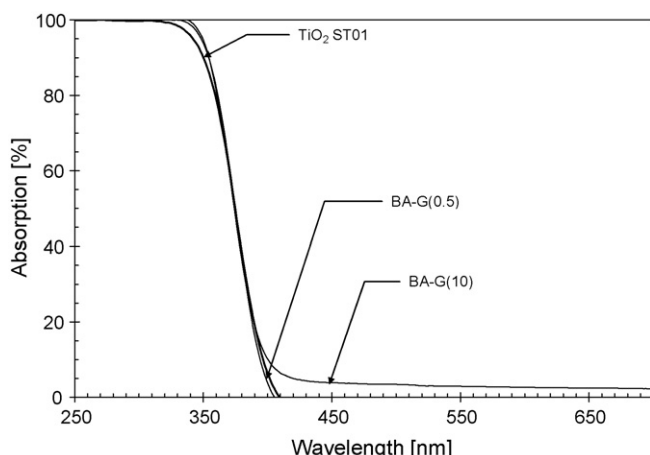


Fig. 4. Diffuse reflectance spectra of TiO₂ ST-01 and B-doped prepared by grinding anatase with H₃BO₃.

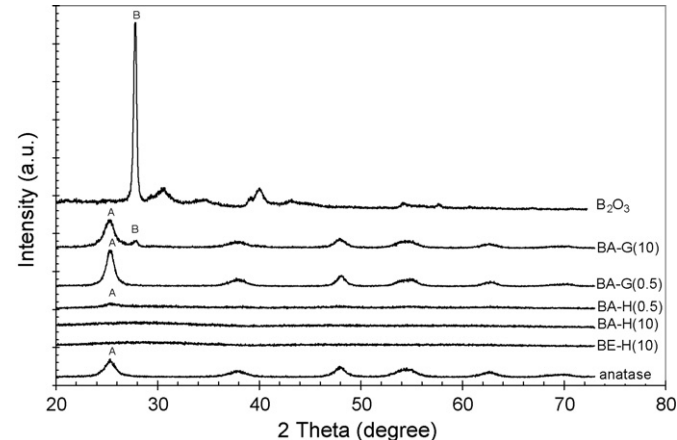


Fig. 5. XRD pattern of pure TiO₂ and selected photocatalysts modified with (C₂H₅O)₃B or H₃BO₃.

All our samples obtained by grinding of ST-01 with boron compounds still contained the anatase phase. The XRD pattern of samples BA-G(10) and BE-G(10) shows diffraction lines attributed to the diboron trioxide phase besides the peak due to anatase (see Fig. 5). Chen et al. found that appearance of separate boron phase is related not only to the calcination temperature but also the molar ratio of B to Ti. For samples with $R_B = 10$ the diboron trioxide crystal appeared during calcination over 600 °C. When R_B was 20, the B₂O₂ phase emerged at 500 °C. In our study, B₂O₃ structure was observed for samples prepared by grinding with 10 wt.% of boron in two different precursors. Apparently 0.5 wt.% was not enough to form clearly evident B₂O₃.

For samples in the anatase form, the average crystallite size (L) was calculated as a function of peak width, specified as the full width at half maximum (FWHM) peak intensity based on Scherrer's formula. For all the B-TiO₂ samples prepared by grinding, L ranged from 10 to 14 nm. Measured BET surface area, see Table 1, of samples BE-H series changed from 208, 237 and 269 to 190 m²/g, as triethyl ester boric acid amount increased from 0.5 to 10 wt.%. The specific surface of pure TiO₂ obtained by TIP hydrolysis followed by calcination at 450 °C was only 180 m²/g. BET surface area for BA-H(0.5) and BA-H(10) samples equals to 190 and 330 m²/g. Such a unique surface area probably results from crystallization hindering by 10 wt.% of boric acid. Similar tendency was observed by Chen et al. [27]. BET surface area of samples prepared by Chen et al. by calcination at 500 °C, changed from 95.4, 99.3, 101.4, 108.9, and 119.6 m²/g to 110.4 m²/g when R_B was equal to 0, 1, 3, 5, 10 and 20, respectively [27].

For ST-01 measured BET surface area was 211 m²/g which is below than specific surface area specified by Ishihara Sangyo. All samples, prepared by grinding of ST-01 with dopant, followed by calcination, had lower surface than original TiO₂. For samples BE-G(0.5), BE-G(10) and BA-G(0.5) BET surface area are 158, 160 and 163 m²/g, respectively. In case of sample BA-G(10) surface area decreased to 82 m²/g. Obtained results indicate that addition of (C₂H₅O)₃B or H₃BO₃ contributed to shrinkage of surface area through particle agglomeration and/or pores closing.

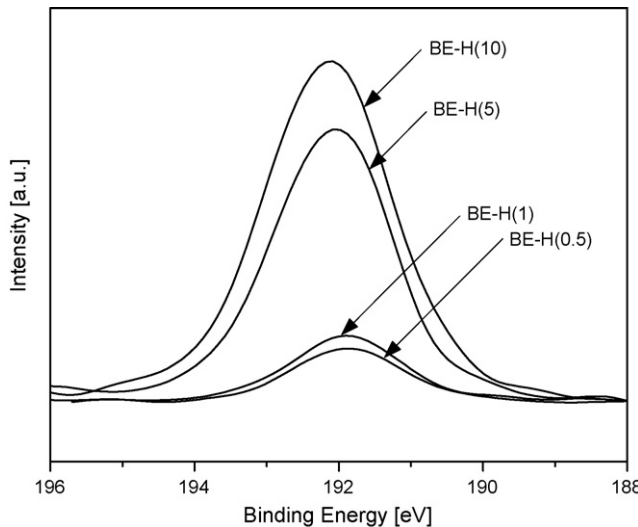


Fig. 6. B 1s comparison BE-H samples, normalized at 188 eV.

To investigate the chemical states of C and B atoms incorporated into TiO_2 the binding energies were measured by X-ray photoemission spectroscopy. Fig. 6 shows the XPS B 1s spectra of B-TiO₂ photocatalysts prepared by hydrolysis of TIP in the presence of boric acid triethyl ester (from 0.5 to 10 wt.%). Boron and carbon content determined by XPS analysis, as well as sample composition, are presented in Table 2. For B-TiO₂, the B 1s appeared at around 192 eV. For pure TiO₂, the B 1s peak does not appear. The peak area of B 1s increased with the increase of the dopant amount. The binding energy of B 1s peak for samples with bigger amount of the dopant (5 and 10 wt.%) is about 0.3 eV greater compared to BE observed for samples containing lower amount of the dopant (0.5 and 1 wt.%), see Fig. 6. The standard binding energy of B 1s in B_2O_3 or H_3BO_3 equals to 193.0 eV (B–O bond) and in TiB_2 equals to 187.5 eV (B–Ti bond) [27]. Our observed peak, around 192 eV, could be attributed to the B–O–Ti bond. For increasing boron content, the dominance of the B–O bond (B_2O_3) was observed. It was indicated by the shift of binding energy for B 1s peak to higher

BE value for samples with greater B content. Also the presence of O 1s peak around 533 eV confirmed the presence of B–O bonds. FT-IR and XPS results obtained by Chen et al. [27] revealed that the doped boron was present as the form of B^{3+} in B-doped TiO₂ samples, forming a possible chemical structure like Ti–O–B, which was confirmed in our investigation. The peak B 1s was also observed after Ar^+ ion etching of the sample. The atomic content of boron atoms on surfaces of BE-H(0.5) sample increased from 1.71 to 2.31 at.% after Ar^+ etching.

Comparison of XPS spectra for O 1s region for samples containing 0.5 and 10 wt.% of boron is provided in Fig. 7. Samples containing 0.5 wt.% of boron clearly exhibit 530.1 eV binding energy for ground samples, while 530.4 eV for a catalyst obtained by the sol–gel method. Boron contact with titanium dioxide molecules is much more intimate in the sol–gel method than that resulting from interparticles interactions during grinding. Thus, Ti–O–B bonds can be formed, as indicated by the binding energy shift clearly seen in Fig. 7A. A similar effect can be seen for the elevated content of boron (10 wt.%), see Fig. 7B. Additionally, another 532.4 eV peak, which can be assigned to B_2O_3 , for the ground catalyst spectra is evident. Although the sol–gel catalyst spectra do not have an additional peak, the asymmetry of the peak around 532 eV speaks for appearance of B_2O_3 . For samples BE-G(10) and BA-G(10), presence of diboron oxide was confirmed by both XRD and XPS analyses.

In all B-doped and pure TiO₂ samples we observed the peak attributed to C 1s at around 289–284 eV. In most cases, the C 1s region consists of three peaks. The first peak (~288.9 eV) is related to COOH groups bonds, the second peak (~286 eV) to C–OH bonds and the third peak (~284.6 eV) is related to C–C aromatic bonds. For two samples – BE-G(10) and BA-G(10) – a thin film of conductive carbon was observed. As a result, additional group of carbon peaks at around 284–282 eV were noticeable at XPS spectrum. The XPS spectra – region corresponding to C 1s – for samples BA-G(0.5) and BA-G(10) are shown in Fig. 8. One should notice the differences in binding energy corresponding to the peaks in Fig. 8A and B.

Table 2
Atomic composition of B-TiO₂ catalysts

Sample no.	Amount of dopant (wt.%)	XPS-determined content (at.%)		Composition
		C	B	
BE-H(0.5)	0.5	8.38	1.71	$\text{TiO}_{2.47}\text{B}_{0.06}\text{C}_{0.32}$
BE-H(1)	1	8.42	1.82	$\text{TiO}_{2.72}\text{B}_{0.07}\text{C}_{0.35}$
BE-H(5)	5	13.14	6.86	$\text{TiO}_{3.1}\text{B}_{0.35}\text{C}_{0.68}$
BE-H(10)	10	6.92	8.66	$\text{TiO}_{3.1}\text{B}_{0.42}\text{C}_{0.33}$
BE-G(0.5)_A ^a	0.5	18.54	3.21	$\text{TiO}_{2.9}\text{B}_{0.17}\text{C}_{0.96}$
BE-G(0.5)_B ^a	0.5	12.20	2.83	$\text{TiO}_{3.7}\text{B}_{0.16}\text{C}_{0.7}$
BE-G(0.5)_C ^a	0.5	14.12	2.29	$\text{TiO}_{2.83}\text{B}_{0.11}\text{C}_{0.67}$
BE-G(10)	10	18.43	12.33	$\text{TiO}_{3.85}\text{B}_{0.87}\text{C}_{1.45}$
BA-H(0.5)	0.5	19.13	1.14	$\text{TiO}_{2.62}\text{B}_{0.05}\text{C}_{0.9}$
BA-H(10)	10	14.28	9.11	$\text{TiO}_{3.33}\text{B}_{0.85}\text{C}_{0.54}$
BA-G(0.5)	0.5	10.36	2.32	$\text{TiO}_{2.81}\text{B}_{0.11}\text{C}_{0.47}$
BA-G(10)	10	3.98	24.55	$\text{TiO}_{6.42}\text{B}_{2.59}\text{C}_{0.42}$
Pure TiO_2	No dopant	10.74	ND	$\text{TiO}_{3.7}\text{C}_{0.57}$

ND—below detection limit.

^a Samples having the same composition and made according to identical procedure, prepared independently.

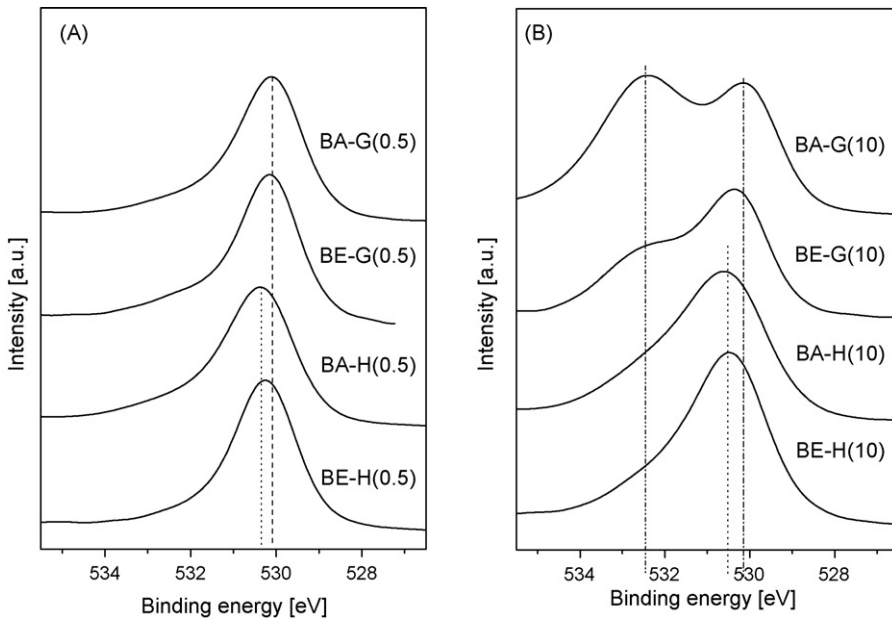


Fig. 7. O 1s comparison of B-TiO₂ samples prepared by different methods: (A) samples containing 0.5 wt.% of boron; (B) samples containing 10 wt.% of boron.

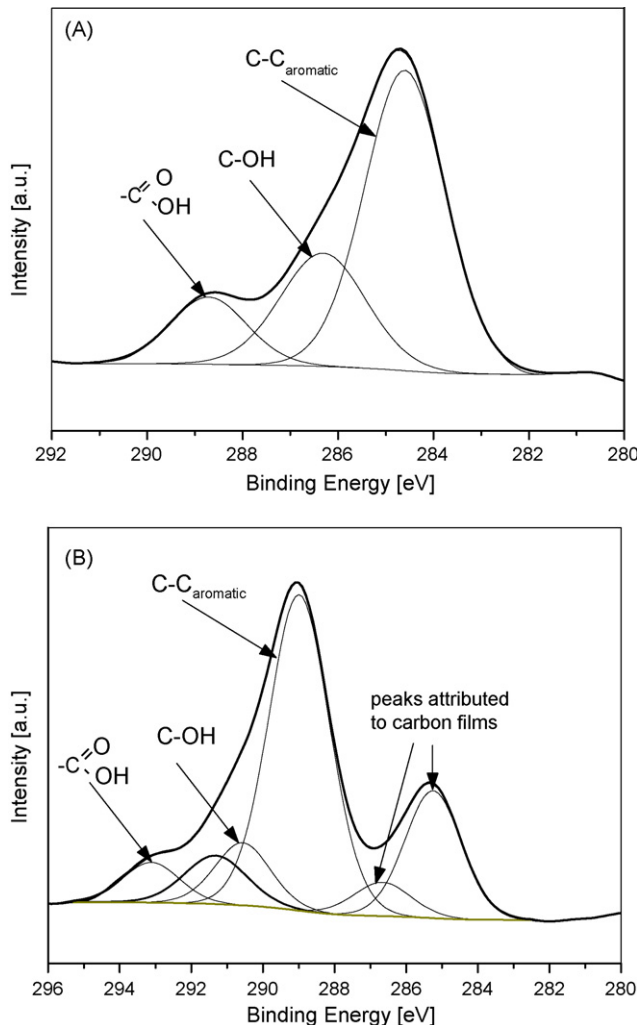


Fig. 8. XPS spectra of C 1s peak: (A) sample BA-G(0.5); (B) sample BA-G(10). Difference in binding energy can be observed resulting from the presence of conductive carbon layer in catalyst represented in (B).

Spectrum in Fig. 8A was made for material having nonconductive surface layer, concentrating electrical charge, which results in 5.02 eV binding energy shift. Thin carbon film allows to drain the electrical charge, which is the case with the catalyst represented by spectrum in Fig. 8B.

The C–C peak results from the presence of remaining alkoxy groups originating from the sol–gel preparation [28]. While the boron content increased with an increasing amount of the dopant, we could not observe the same correlation for the carbon. We could expect that samples prepared by hydrolysis of TIP in the presence of boric acid ester include higher amount of carbon, originating either from titanium precursor or organic dopant. However, XPS analysis indicates sample BA-H(0.5) – prepared by hydrolysis of TIP in the presence of boric acid – as the sample containing more carbon (19.13 at.%). In this sample carbon could originate only from the organic titanium precursor.

Photocatalytic activity of B-doped TiO₂ powders was estimated by measuring the decomposition rate of phenol in the presence of UV or vis irradiation. Pure TiO₂ synthesized by the sol–gel method without any dopant and ST-01 was used as the reference system. It was found that phenol concentration remained stable after 1 h of stirring without illumination in the presence of obtained powders. Fig. 9 shows the results of phenol degradation under UV irradiation in the presence of TiO₂ modified with boric acid triethyl ester synthesized by sol–gel method and by grinding. In the presence of ultraviolet irradiation, all powders prepared by the sol–gel method with boric acid triethyl ester exhibited lower photoactivity than pure TiO₂ (see Fig. 9A), while both photocatalysts prepared by grinding with boric acid triethyl ester revealed similar photoactivity with respect to pure TiO₂ ST-01 (Fig. 9B). This result suggests that doping of B atoms into TiO₂ particles does not improve photocatalytic activity for oxidation of phenol under UV light.

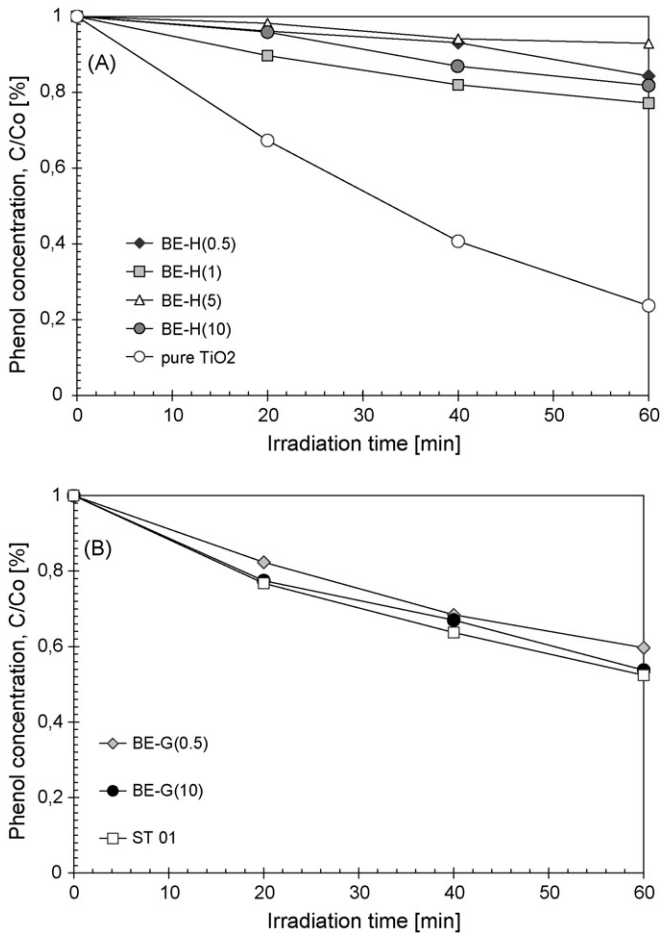


Fig. 9. Photoactivity under UV light of B-TiO₂ modified with boric acid triethyl ester prepared by (A) sol-gel method; (B) grinding with a dopant. Experimental conditions: $C_0 = 0.21 \text{ mM}$; $m (\text{TiO}_2) = 125 \text{ mg}$, $T = 10^\circ\text{C}$, $Q_{\text{air}} = 5 \text{ l/h}$, $\lambda < 400 \text{ nm}$.

Activity of BE-H and BE-G series under visible light ($\lambda > 400 \text{ nm}$) are shown in Fig. 10. All photocatalysts prepared by hydrolysis of TIP in the presence of boric acid triethyl ester revealed the same photoactivity under visible light comparable to that of pure TiO₂. Better photoactivity under visible light was observed only for B-TiO₂ prepared by grinding of ST-01 with boric acid triethyl ester. In the presence of BE-G(0.5) and BE-G(10) samples, phenol was degraded in 62 and 46% after 60 min of irradiation, respectively (see Fig. 10B). It means that the highest photoactivity was observed for lower dopant amount (0.5 wt.%). However, we did not investigate the influence of the dopant amount between 0.5 and 10 wt.%.

Figs. 11 and 12 show photoactivity of TiO₂ modified with boric acid under UV and vis light, respectively. Our measurements revealed that application of inorganic dopant as a boron source resulted in lower photoactivity of obtained B-TiO₂ than pure TiO₂ under UV light. All obtained powders in BA series have almost the same photoactivity under visible light, though sample BA-H(10) shows better absorption in visible region than pure titanium dioxide (see Fig. 3).

In reductive environment, nicotinamide adenine dinucleotide (NADH) regeneration under UV light irradiation, Chen et al. [27] observed better photocatalytic activity of B-doped

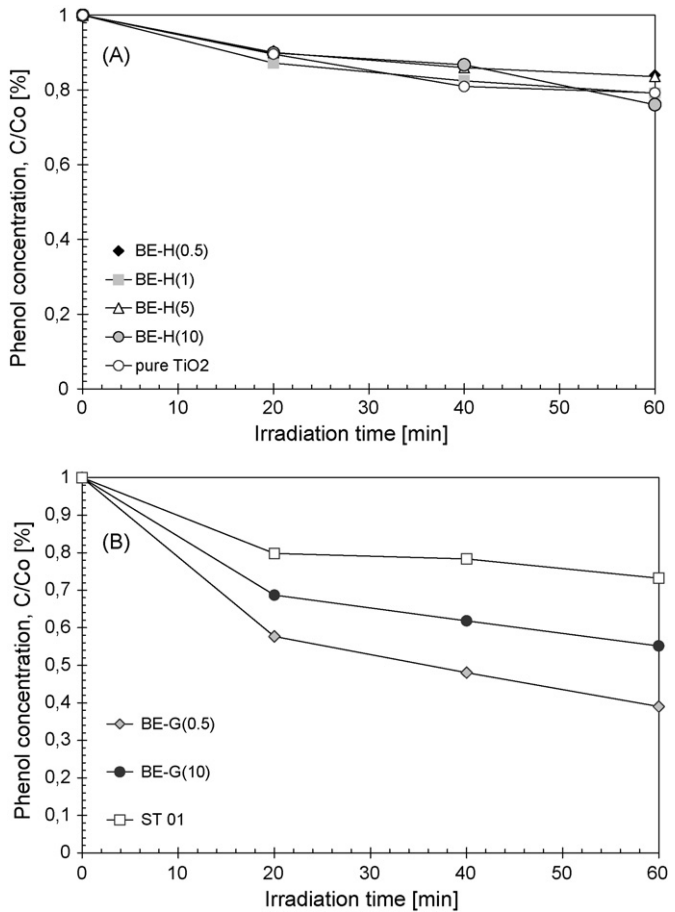


Fig. 10. Photoactivity under visible light ($\lambda > 400 \text{ nm}$) of B-TiO₂ modified with boric acid triethyl ester prepared by (A) sol-gel method; (B) grinding with a dopant. Experimental conditions: $C_0 = 0.21 \text{ mM}$; $m (\text{TiO}_2) = 125 \text{ mg}$, $T = 10^\circ\text{C}$, $Q_{\text{air}} = 5 \text{ l/h}$, $\lambda > 400 \text{ nm}$.

TiO₂ than pure TiO₂. NADH was reproduced in 94% when the molar ratio of B to Ti was 5%. Titanium tetra-n-butyl oxide and H₃BO₃ were used as TiO₂ and boron precursors. In our investigation, boric acid triethyl ester exhibited a better boron source than boric acid to enhance photoactivity.

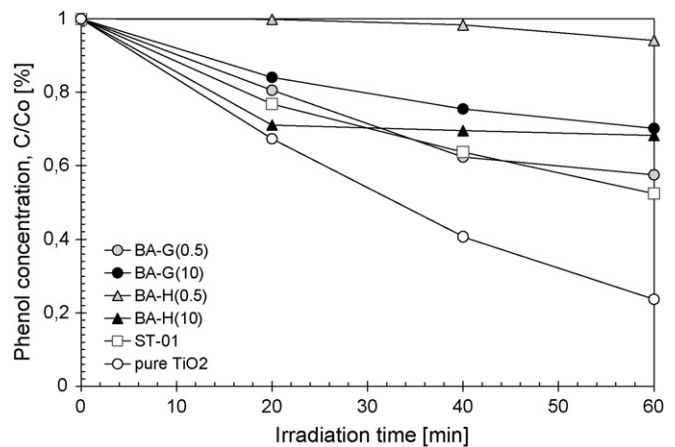


Fig. 11. Photoactivity under UV light of B-TiO₂ modified with H₃BO₃ prepared by sol-gel method and by grinding with dopant. Experimental conditions: $C_0 = 0.21 \text{ mM}$; $m (\text{TiO}_2) = 125 \text{ mg}$, $T = 10^\circ\text{C}$, $Q_{\text{air}} = 5 \text{ l/h}$, $\lambda < 400 \text{ nm}$.

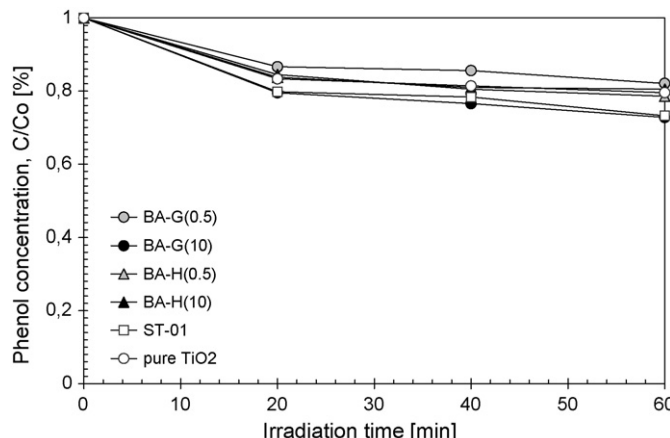


Fig. 12. Photoactivity under visible light ($\lambda > 400$ nm) of B-TiO₂ modified with H₃BO₃ prepared by sol-gel method and by grinding with a dopant. Experimental conditions: $C_0 = 0.21$ mM; m (TiO₂) = 125 mg, $T = 10^\circ\text{C}$, $Q_{\text{air}} = 5$ l/h, $\lambda > 400$ nm.

Geng et al. [24] in theoretical calculations considered three approaches in doping: (I) one of the Ti atoms is substituted by boron, (II) interstitial boron doping and (III) one of oxygen atoms is replaced by a boron atom. They found that in systems I and II the doped B atom should not appreciably modify density states (DOS) near the Fermi surface. Such a kind of doping can form deep impurities level in the energy spectrum. The induced electronic level is buried at the bottom of the valence band and doping would not shift the absorption edge [24]. However, for case III, the DOS projections for the B impurities atom not only contribute to the low-energy part (~ -8 eV), but also to the high-energy portion (-2 eV), close to the Fermi surface. Because of the strong electronegativity of B compared to the neighbor O atom, there appears appreciable electron transfer from B to O, and from Ti to B, therefore the impurity would affect the charge density of the nearest and the second-nearest, and even beyond the second-nearest neighbors. The effect of the impurity would not be localized. Geng et al. [24] compared the total energies for the three doping cases with respect to relative structure stabilities. According to Geng et al. [24] calculations, the O substitution may be responsible for the observed photocatalytic activity of samples BE-G(0.5) and BE-G(10). However, photoactivity of our samples under visible light could originate from both carbon and boron presence, see also Refs. [29,30] regarding the role of carbon.

Catalysts which exhibited best photoactivity in visible light were prepared by grinding TiO₂ with 0.5 and 10 wt.% of boric acid triethyl ester. Phenol degradation under visible light was 35 and 18% more efficient for samples BE-G(0.5) and BE-G(10), respectively, than in the presence of ST-01 powder. Sample BE-G(0.5) was prepared independently three times (therefore in Table 2 is marked as BE-G(0.5)_A, BE-G(0.5)_B and BE-G(0.5)_C). All samples prepared by grinding of ST-01 with 0.5% of boric acid triethyl ester revealed similar photoactivity: phenol was degraded in 56–62% after 60 min of irradiation, although surface carbon and boron content differed within 24 and 18%. Such a result allows to look

favorably to possible applications of the catalyst and its preparation method.

Sample BE-G(0.5) is in anatase form and its surface area equals to 160 m²/g. The absorption tails of BE-G(0.5) and BE-G(10) both extended over 700 nm. As shown in Fig. 2, the visible-light absorption of BE-G(0.5) was higher than that of BE-G(10), and the visible-light activity of BE-G(0.5) was better than that of BE-G(10). On the other side, sample BE-H(10), which revealed highest visible-light absorption, was not active under visible light. Visible-light absorption of sample BE-H(10) could result from defects and/or impurities (e.g. carbon which presence was evidenced by dark-brownish color).

The weaker visible-active sample BE-G(10) is richer in boron than sample BE-G(0.5) (see Table 2). The presence of B₂O₃ probably decreased photoactivity in visible light, and higher activity of sample BE-G(0.5) could be attributed to Ti–O–B boron structure. Moreover, visible-light activity of sample BE-G(0.5) could be enhanced by high content of Ti³⁺ ions. Ti³⁺ to Ti⁴⁺ ratio equal to 0.096 for sample BE-G(0.5) was higher than for most other samples.

4. Conclusions

New boron-doped titanium dioxide catalysts were prepared using the sol-gel, and mortar and pestle pulverization and mixing preparation procedures.

1. Our investigation confirmed prediction made by Xu et al. that boron doping can result in absorption of visible light and that B-TiO₂ can be active in the presence of visible light. Only catalysts prepared by grinding and mixing titanium dioxide with boric acid triethyl ester were active for $\lambda > 400$ nm.
2. Contrary to the literature data, obtained B-TiO₂ did not reveal better activity under UV light in photooxidation of phenol compared to pure TiO₂.
3. Both carbon and boron showed beneficial influence on the photodegradation efficiency in visible light activity. Ti–O–B species were shown to contribute to the photoactivity.
4. Boron doping during TiO₂ catalyst preparation by the sol-gel method inhibited transformation from amorphous to the anatase structure.
5. Addition of more boron dopant (e.g. 10%) resulted in appearance of diboron trioxide phase. B₂O₃, which presence was confirmed by XRD and XPS analysis, lowers the photocatalytic activity, therefore, its formation should be avoided.

Acknowledgments

This research was supported by Polish Ministry of Science and Higher Education (Contract No.: N205 077 31/3729). Dr. Beata Tryba (Department of Water Technology and Environmental Engineering, Szczecin University of Technology) and Dr. Maria Gazda (Department of Solid State Physics, Gdańsk University of Technology) are gratefully acknowledged for assistance in UV-vis spectroscopy and XRD analysis.

References

- [1] A. Fujishima, K. Honda, *Nature* 283 (1972) 37–38.
- [2] S.N. Frank, A.J. Bard, *J. Am. Chem. Soc.* 99 (1977) 303.
- [3] A. Fujishima, X. Zhang, *C.R. Chim.* 9 (2006) 750–760.
- [4] M.R. Hoffmann, S.T. Martin, W. Choi, D.W. Bahnemann, *Chem. Rev.* 95 (1995) 69–96.
- [5] M. Anpo, *Pure Appl. Chem.* 72 (2000) 1787–1792.
- [6] H. Yamashita, M. Harada, J. Misaka, M. Takeuchi, Y. Ichihashi, F. Goto, M. Ishida, T. Sasaki, M. Anpo, *J. Synchrotron. Rad.* 8 (2001) 569–571.
- [7] S. Klosek, D. Raftery, *J. Phys. Chem. B.* 105 (2001) 2815–2819.
- [8] H. Yamashita, M. Harada, J. Misaka, M. Takeuchi, K. Ikeue, M. Anpo, *J. Photochem. Photobiol. A: Chem.* 148 (2002) 257–261.
- [9] I. Nakamura, N. Negishi, S. Kutsuna, T. Ihara, S. Sugihara, K. Takeuchi, *J. Mol. Catal. A: Chem.* 161 (2000) 205–212.
- [10] K. Takeuchi, I. Nakamura, O. Matsumoto, S. Sugihara, M. Ando, T. Ihara, *Chem. Lett.* 29 (2000) 1354–1355.
- [11] R. Asahi, T. Morikawa, T. Ohwaki, K. Aoki, Y. Taga, *Science* 293 (2001) 269–271.
- [12] T. Morikawa, R. Asahi, T. Ohwaki, K. Aoki, Y. Taga, *Jpn. J. Appl. Phys.* 40 (2001) L561–L563.
- [13] H. Irie, Y. Watanabe, K. Hashimoto, *J. Phys. Chem. B.* 107 (2003) 5483–5486.
- [14] C. Chen, H. Bai, S. Chang, C. Chang, W. Den, Preparation of N-doped TiO₂ photocatalyst by atmospheric pressure plasma process for VOCs decomposition under UV and visible light sources, *J. Nanopart. Res.* 9 (2007) 365–375.
- [15] S. Sato, R. Nakamura, S. Abe, *Appl. Catal., A* 284 (2005) 131–137.
- [16] T. Ohno, T. Mitsui, M. Matsumura, *Chem. Lett.* 32 (2003) 364–365.
- [17] T. Umebayashi, T. Yamaki, S. Tanaka, K. Asai, *Chem. Lett.* 32 (2003) 330–331.
- [18] T. Tachikawa, S. Tojo, K. Kawai, M. Endo, M. Fujitsuka, T. Ohno, K. Nishijima, Z. Miyamoto, T. Majima, *J. Phys. Chem. B* 108 (2004) 19299–19306.
- [19] M. Katoh, H. Aihara, T. Hrikawa, T. Tomida, *J. Colloid Interface Sci.* 298 (2006) 805–809.
- [20] O. Diwald, T.L. Thompson, T. Zubkov, E.G. Goralski, S.D. Walck, J.T. Yates Jr., *J. Phys. Chem. B* 108 (2004) 6004–6008.
- [21] T. Ohno, M. Akiyoshi, T. Umebayashi, K. Asai, T. Mitsui, M. Matsumura, *Appl. Catal., A* 265 (2004) 115–121.
- [22] A. Zaleska, P. Gorska, J.W. Sobczak, J. Hupka, *Appl. Catal., B* 76 (2007) 1–8.
- [23] T. Xu, C. Song, Y. Liu, G. Han, *Zhejiang Univ. Sci. B* 7 (2006) 299–303.
- [24] H. Geng, S. Yin, X. Yang, Z. Shuai, B. Liu, *J. Phys.: Condens. Matter* 18 (2006) 87–96.
- [25] S. Moon, H. Mametsuka, S. Tabata, E. Suzuki, *Catal. Today* 58 (2000) 125–132.
- [26] W. Zhao, W. Ma, C. Chen, J. Zhao, Z. Shuai, *J. Am. Chem. Soc.* 126 (2004) 4782.
- [27] D. Chen, D. Yang, Q. Wang, Z. Jiang, *Ind. Eng. Chem. Res.* 45 (2006) 4110–4116.
- [28] H. Jensen, A. Soloviev, Z. Li, E.G. Sogaard, *Appl. Surf. Sci.* 246 (2005) 239–249.
- [29] C. Lettmann, K. Hildebrand, H. Kisch, W. Macyk, W.F. Maier, *Appl. Catal., B* 32 (2001) 215–227.
- [30] B. Tryba, T. Tsumura, M. Janus, A.W. Morawski, M. Inagaki, *Appl. Catal., B* 50 (2004) 177–183.